VI International Conference on Computational Methods for Coupled Problems in Science and Engineering
COUPLED PROBLEMS 2015
B. Schrefler, E. Oñate and M. Papadrakakis(Eds)

SIMULATION OF SELF-HEALING PROCESSES IN MICROCAPSULE BASED SELF-HEALING POLYMERIC SYSTEMS

Steffen Specht*, Joachim Bluhm* and Jörg Schröder*

*Institute of Mechanics
University of Duisburg-Essen
Universitätsstr. 15, 45141 Essen, Germany
e-mail: steffen.specht@uni-due.de, web page: http://www.uni-due.de/mechanika

Key words: Self-healing materials, Theory of Porous Media, Phase transition

Abstract. Self healing materials are becoming more and more important for the construction of mechanical components due to their ability to detect and heal failures and cracks autonomously. Especially in polymers and polymer-composites, where the component can loose a high rate of strength and durability due to micro cracks, those damages are nearly impossible to repair from outside. Thus, self healing ability is a very effective approach to extend the lifetime of polymer-made components.

In view of the numerical simulation of such self healing effects we develop a thermodynamically consistent macroscopic 5-phase model within the theoretical framework of the Theory of Porous Media. The model consists of the following different phases: solid (matrix material) with dispersed catalysts, liquid (healing agents), healed material and gas (air inside the cracks). The increase of damage is driven by a discontinuous damage evolution equation. Furthermore, a mass exchange between the liquid-like healing agents and the solid-like healed material, i.e. the change of the aggregate state from liquid healing to solid healed material, describes the healing process. The onset of the healing process is associated with the break open of the microcapsules in connection with the subsequent motion of the liquid healing agents. A numerical example of the simulation of damage and healing processes in polymers, is presented in order to show the applicability of the model.

1 INTRODUCTION

Self-healing materials have the ability to repair damages autonomously, i.e., no manual intervention is necessary. Such a behavior can be realized for example with a multiphase material, which consists of a solid matrix material (epoxy) with dispersed catalysts (Grubbs' catalysts) and microcapsules, which are filled with liquid healing agents (dicyclopentadiene). If a crack propagates through the body, the capsules break open and release the healing agents into the crack, where they react with the catalysts, polymerize and close the crack, cf. [1]. Such a self-healing approach is very useful for components where the detection and repair is very difficult

and/or very costly like in aerospace applications. For an overview of different self-healing materials can be found in [2], whereas [3] and [4] show the different principles of self-healing.

In view of the numerical simulation of self-healing materials, several examples can be found in literature. Some of these publications are listed in the following:

Self healing effects of polymers in an analytical manner where analyzed by [5]. Regarding fiber reinforced composites the self healing behavior was investigated and simulated by [6–8]. In view of the development of thermodynamically consistent models it is referred to [9–11]. In [12] the simulations base on Continuum Damage Mechanics (CDM), and [13] taking continuous damage and healing variables into account. The model of [14] is based on the Mixture Theory.

In this contribution we focus on the numerical simulation of self-healing materials using the Theory of Porous Media, as described in the following.

2 THEORY

For the description of coupled multiphase problems, the Theory of Porous Media (TPM) can be used. This macroscopic continuum mechanical approach is basically a combination of the Mixture Theory and Concept of Volume Fractions.

Using the the Mixture Theory, one is able to describe, for example, all κ constituents φ^α of a multiphase problem by their own independent motion function. Furthermore, the superposition of the phases is assumed, i.e., all different constituents appear in a spatial point $\mathbf{x}$ simultaneously, see Figure 1. Due to that, all geometrical and physical quantities are defined as statistically averages of the real quantities in the observed body.

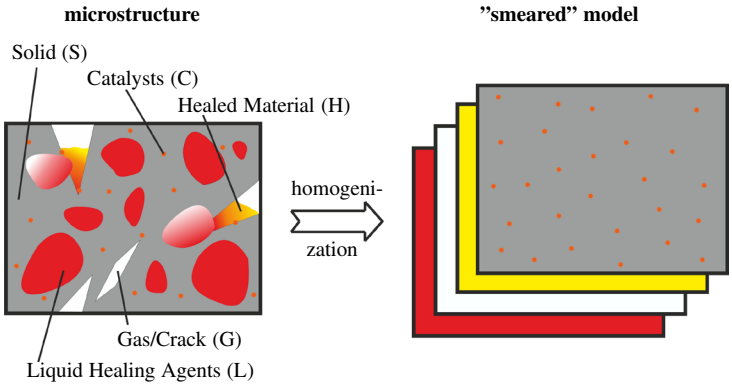

Figure 1: Homogenization of the microstructure.

Additionally, with help of the concept of volume fractions, the different constituents φ^α in a material point $\mathbf{x}$ can be identified by the volume fraction of the corresponding phase, which relates the real quantities with the partial quantities. For example, the partial density ρ^α of a certain constituent can be directly related to its real density $\rho^{\alpha\mathrm{R}}$ using the corresponding volume

fraction $\mathrm{n}^\alpha = \mathrm{dv}^\alpha/\mathrm{dv}$, such that $\rho^\alpha = \mathrm{n}^\alpha \rho^{\alpha\mathrm{R}}$. The sum over all κ volume fractions n^α in a material point $\mathbf{x}$ is restricted by the so called saturation condition

$$\sum_{\alpha=1}^{\kappa} \mathrm{n}^\alpha = 1\,. \tag{1}$$

For a detailed introduction into the Theory of Porous Media, the interested reader is referred to the publications [15–20].

3 SIMPLIFIED FIVE-PHASE MODEL

In the following the developed five phase model for the description of the considered self healing material will be presented. It consists of the solid matrix material (S) with dispersed catalysts (C), the liquid healing agents (L), the solid like healed material (H), and the gas phase (G), which represents the air. In order to build up the model, some assumptions and simplifications are made: 1) the whole is treated as isothermal; 2) dynamic effects are neglected; 3) mass transition will be considered only between the liquid like healing agents and the solid like healed material, in order to describe the phase transition of the healing material; 4) all phases are assumed to be incompressible ($\rho^{\alpha\mathrm{R}} = \text{const.}$), except the gas phase which is compressible ($\rho^{\mathrm{GR}} \neq \text{const.}$); 5) the volume fraction of the catalysts is neglected with respect to the saturation condition, due to the fact that it is very small in comparison with the other phases; 6) the velocities of the solid and the solidified healed material are assumed to be identical, except at an initial solid motion, i.e., before the healing mechanism is activated. This leads to a multiplicative decomposition of the deformation gradient, depicted in Figure 2, in the form

$$\mathbf{F}_\mathrm{S} = \mathrm{Grad}\,\boldsymbol{\chi}_\mathrm{S} = \frac{\partial \boldsymbol{\chi}_\mathrm{S}}{\partial \mathbf{X}_\mathrm{S}} = \mathbf{F}_\mathrm{H}\,\mathbf{F}_{\mathrm{S}0}\,, \tag{2}$$

which can be found in [21–23]. Due to the multiplicative decomposition of the deformation gradient, three different right Cauchy-Green deformation tensors (corresponding to the whole deformation, the deformation before and after the healing is activated) are available,

$$\mathbf{C}_\mathrm{S} = \mathbf{F}_\mathrm{S}^\mathrm{T}\,\mathbf{F}_\mathrm{S}\,, \qquad \mathbf{C}_{\mathrm{S}0} = \mathbf{F}_{\mathrm{S}0}^\mathrm{T}\,\mathbf{F}_{\mathrm{S}0}\,, \qquad \hat{\mathbf{C}}_\mathrm{H} = \mathbf{F}_\mathrm{H}^\mathrm{T}\,\mathbf{F}_\mathrm{H}\,. \tag{3}$$

3.1 Field Equations

Considering the above mentioned assumptions and simplifications, the field equations are given by the balance equation of mass for the solid, healed material, liquid healing agents, catalysts and gas,

$$(\mathrm{n}^\mathrm{S})'_\mathrm{S} + \mathrm{n}^\mathrm{S}\,\mathrm{div}\,\mathbf{x}'_\mathrm{S} = 0\,, \qquad (\mathrm{n}^\mathrm{H})'_\mathrm{S} + \mathrm{n}^\mathrm{H}\,\mathrm{div}\,\mathbf{x}'_\mathrm{S} = \frac{\hat{\rho}^\mathrm{H}}{\rho^{\mathrm{HR}}}\,, \tag{4}$$

$$(\mathrm{n}^\mathrm{L})'_\mathrm{L} + \mathrm{n}^\mathrm{L}\,\mathrm{div}\,\mathbf{x}'_\mathrm{L} = -\frac{\hat{\rho}^\mathrm{H}}{\rho^{\mathrm{LR}}}\,, \qquad \mathrm{n}^\mathrm{S}\,(\mathrm{c}^\mathrm{C})'_\mathrm{S} - \mathrm{div}\,(\mathrm{n}^\mathrm{S}\,\mathrm{c}^\mathrm{C}\,\mathbf{w}_{\mathrm{CS}}) = \hat{\rho}^\mathrm{C}\,,$$

$$(\mathrm{n}^\mathrm{G})'_\mathrm{G} + \mathrm{n}^\mathrm{G}\,\mathrm{div}\,\mathbf{x}'_\mathrm{G} + \frac{\mathrm{n}^\mathrm{G}}{\rho^{\mathrm{GR}}}\,(\rho^{\mathrm{GR}})'_\mathrm{G} = 0\,,$$

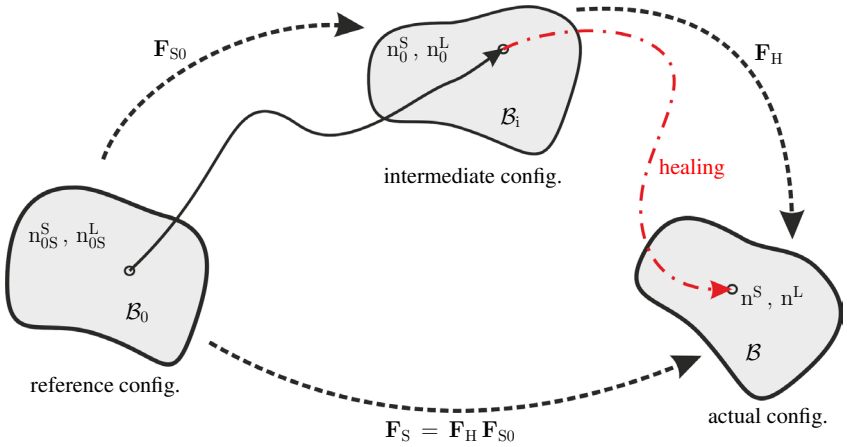

Figure 2: Illustration of the multiplicative decomposition of the deformation gradient of the solid phase.

the balance equations of momentum for the mixture as well as for the liquid and gas phases,

$$\operatorname{div} \mathbf{T}^{\mathrm{SHLCG}} + \rho^{\mathrm{SHLCG}} \mathbf{b} = -\hat{\rho}^{\mathrm{H}} \mathbf{w}_{\mathrm{LS}} , \qquad \operatorname{div} \mathbf{T}^{\mathrm{L}} + \rho^{\mathrm{L}} \mathbf{b} = -\hat{\mathbf{p}}^{\mathrm{L}} , \qquad \operatorname{div} \mathbf{T}^{\mathrm{G}} + \rho^{\mathrm{G}} \mathbf{b} = -\hat{\mathbf{p}}^{\mathrm{G}} , \tag{5}$$

and the material time derivative of the saturation condition with respect to the solid phase,

$$\operatorname{div} (\mathrm{n}^{\mathrm{L}} \mathbf{w}_{\mathrm{LS}} + \mathrm{n}^{\mathrm{G}} \mathbf{w}_{\mathrm{GS}} + \mathbf{x}_{\mathrm{S}}') + \frac{\mathrm{n}^{\mathrm{G}}}{\rho^{\mathrm{GR}}} (\rho^{\mathrm{GR}})_{\mathrm{G}}' - \hat{\rho}^{\mathrm{H}} (\frac{1}{\rho^{\mathrm{HR}}} - \frac{1}{\rho^{\mathrm{LR}}}) = 0 . \tag{6}$$

With the symbol $(\dots)_\alpha'$, the material time derivative of the expression with respect to the corresponding constituent φ^α is indicated and $\hat{(\dots)}$ denotes the direct production terms, in this case of mass and momentum, respectively. The relative velocities $\mathbf{w}_{\zeta\mathrm{S}} = \mathbf{x}_\zeta - \mathbf{x}_\mathrm{S}$ $(\zeta = \mathrm{L}, \mathrm{C}, \mathrm{G})$ are the difference velocities between the phases ζ and the solid phase. The value $\mathrm{c}^{\mathrm{C}} \in [0, 1]$ indicates the concentration of catalysts and $\mathbf{T}^\alpha = (\mathbf{T}^\alpha)^{\mathrm{T}}$ are the symmetric Cauchy stress tensors for the different constituents. The expressions $\mathbf{T}^{\mathrm{SHLCG}}$ and ρ^{SHLCG} describe the sum of the corresponding Cauchy stresses and partial densities, respectively, of the individual phases.

3.2 Constitutive Relations

In order to be able to solve the problem, constitutive relations for the stresses and the total production terms of mass and momentum are needed. In the following, just the final equations are given. For the derivation of these equations, it is referred to [24].

The constitutive relations for the Cauchy stresses read

$$\begin{aligned} \mathbf{T}^{\mathrm{SH}} = &- \mathrm{n}^{\mathrm{SH}} \lambda \mathbf{I} + \frac{1}{\mathrm{J_S}} \{ (1 - D^{\mathrm{S}}) [2 \mu^{\mathrm{S}} \mathbf{K}_{\mathrm{S}} + \lambda^{\mathrm{S}} (\log \mathrm{J_S}) \mathbf{I}] + \\ &+ \epsilon^{\mathrm{H}} \mathrm{n}^{\mathrm{H}} \mathrm{J_S} (1 - D^{\mathrm{H}}) [2 \mu^{\mathrm{H}} \mathbf{K}_{\mathrm{H}} + \lambda^{\mathrm{H}} (\log \mathrm{J_H}) \mathbf{I}] \} , \end{aligned} \tag{7}$$

$$\mathbf{T}^{\mathrm{L}} = - \mathrm{n}^{\mathrm{L}} \mathrm{p}^{\mathrm{LR}} \mathbf{I} , \quad \mathbf{T}^{\mathrm{G}} = - \mathrm{n}^{\mathrm{G}} \mathrm{p}^{\mathrm{GR}} \mathbf{I} , \quad \mathbf{T}^{\mathrm{C}} = - \mathrm{n}^{\mathrm{C}} \mathrm{p}^{\mathrm{CR}} \mathbf{I} .$$

In Eq. $(7)_1$, the variables $\mathrm{J_S} = \det \mathbf{F}_\mathrm{S}$ and $\mathrm{J_H} = \det \mathbf{F}_\mathrm{H}$ represent the volume deformations of the solid and healed material, respectively. The expressions $\mathbf{K}_\mathrm{S} = \frac{1}{2}(\mathbf{B}_\mathrm{S} - \mathbf{I})$ and $\mathbf{K}_\mathrm{H} = \frac{1}{2}(\mathbf{B}_\mathrm{H} - \mathbf{I})$ are the Karni-Reiner strain tensors, whereat $\mathbf{B}_\mathrm{S} = \mathbf{F}_\mathrm{S}\mathbf{F}_\mathrm{S}^\mathrm{T}$ and $\mathbf{B}_\mathrm{H} = \mathbf{F}_\mathrm{H}\mathbf{F}_\mathrm{H}^\mathrm{T}$ are the left Cauchy-Green strain tensors of the solid and healed material, and $\mathbf{I}$ is the identity tensor. The material parameters μ^S, μ^H and λ^S, λ^H are the Lamé constants. In order to ensure that the healed material part of the Cauchy stresses get its full influence only if the liquid is completely transformed into healed material, the parameter ϵ^H is chosen such that the product $\epsilon^\mathrm{H}\mathrm{n}^\mathrm{H}$ is equal to one if n^H reaches its maximum. The variables D^S and D^H are damage variables in order to describe the isotropic discontinuous damage behavior of the solid and also the healed material. The so called $(1 - D)$ approach was originally introduced in [25] and further discussed, e.g. in [26, 27]. The Lagrange parameter λ in Eq. $(7)_1$ is defined as

$$\lambda = \mathrm{p}^\mathrm{GR} - \mathrm{p}^\mathrm{h}, \tag{8}$$

where p^GR is the real gas pressure given by the nonlinear gas law

$$\mathrm{p}^\mathrm{GR} = -\Theta\,\mathrm{R}^\mathrm{G}\,\rho_\mathrm{0G}^\mathrm{GR}\,\log\frac{\rho_\mathrm{0G}^\mathrm{GR}}{\rho^\mathrm{GR}} + \mathrm{p}_0^\mathrm{GR}, \tag{9}$$

and an additional pressure p^h, which is alligned to the capillary pressure presented in [28],

$$\mathrm{p}^\mathrm{h} = k_\mathrm{h}^\mathrm{L}\,\mathrm{s}^\mathrm{L}\left[\log\left(\frac{\mathrm{s}_0^\mathrm{L}}{\mathrm{s}^\mathrm{L}} - \mathrm{s}_0^\mathrm{L}\right) - \log\left(1 - \mathrm{s}_0^\mathrm{L}\right)\right]. \tag{10}$$

The absolute temperature is given by Θ, R^G denotes the specific gas constant, $\rho_\mathrm{0G}^\mathrm{GR}$ and p_0^GR are initial real gas density and the initial real gas pressure. The constants k_h^L and s_0^L are material parameters and the liquid saturation $\mathrm{s}^\mathrm{L} = \mathrm{n}^\mathrm{L}/(\mathrm{n}^\mathrm{L} + \mathrm{n}^\mathrm{G})$ is the ratio of liquid with respect to the whole hollow space inside the observed body. Furthermore, the real liquid pressure p^LR, appearing in Eq. $(7)_2$, is given by

$$\mathrm{p}^\mathrm{LR} = \mathrm{p}^\mathrm{GR} + k_\mathrm{h}^\mathrm{L}\left[\log\left(\frac{\mathrm{s}_0^\mathrm{L}}{\mathrm{s}^\mathrm{L}} - \mathrm{s}_0^\mathrm{L}\right) - \log\left(1 - \mathrm{s}_0^\mathrm{L}\right)\right], \tag{11}$$

see also [28]. The pressure part of Eq. $(7)_3$ is the real pressure of catalysts,which is given by

$$\mathrm{p}^\mathrm{CR} = -k^\mathrm{C}\,\log\frac{1}{\mathrm{c}^\mathrm{C}} + \mathrm{p}_0^\mathrm{CR}, \tag{12}$$

whereat the concentration c^C is defined as the quotient of the volume fraction of the catalysts with respect to the volume fraction of the solid $\mathrm{c}^\mathrm{C} = \mathrm{n}^\mathrm{C}/\mathrm{n}^\mathrm{S}$.

For the description of mass exchange between the liquid healing agents and the solid healed material $\hat{\rho}^\mathrm{H}$, see equation $(4)_{2,3}$, the production function proposed in [29] is used and modified such that it depends on the concentration of catalysts,

$$\hat{\rho}^\mathrm{H} = \hat{\rho}_\mathrm{m}^\mathrm{H}\left(\frac{\mathrm{c}^\mathrm{C} - \mathrm{c}_0^\mathrm{C}}{\mathrm{c}_m^\mathrm{C}}\right)^2 \exp\left[1 - \left(\frac{\mathrm{c}^\mathrm{C} - \mathrm{c}_0^\mathrm{C}}{\mathrm{c}_\mathrm{m}^\mathrm{C}}\right)^2\right]. \tag{13}$$

Therein, $\hat{\rho}^{\mathrm{H}}_{\mathrm{m}}$ is the maximum value of $\hat{\rho}^{\mathrm{H}}$, and $\mathrm{c}^{\mathrm{C}}_{0}$ is the maximum value of the concentration. The parameter $\mathrm{c}^{\mathrm{C}}_{\mathrm{m}}$ defines the value of concentration where $\hat{\rho}^{\mathrm{H}}$ becomes its maximum. Due to the fact that the amount of catalysts decreases in areas where healing occur, the total production term of mass for the catalysts $\hat{\rho}^{\mathrm{C}}$ in Eq. $(4)_4$ is set to be a negative and constant value.

Furthermore, due to the evaluation of the entropy inequality, the direct production terms of momentum for liquid and gas are given by

$$\begin{aligned} \hat{\mathbf{p}}^{\mathrm{L}} &= \lambda \operatorname{grad} \mathrm{n}^{\mathrm{L}} - \mathrm{p}^{\mathrm{h}} \operatorname{grad} \mathrm{n}^{\mathrm{G}} + \hat{\mathbf{p}}^{\mathrm{L}}_{\mathrm{E}} \,, \\ \hat{\mathbf{p}}^{\mathrm{G}} &= \left(\lambda + \mathrm{p}^{\mathrm{h}} \right) \operatorname{grad} \mathrm{n}^{\mathrm{G}} - \hat{\mathbf{p}}^{\mathrm{G}}_{\mathrm{E}} \,. \end{aligned} \tag{14}$$

In Eq. (14) the vectors $\hat{\mathrm{p}}^{\mathrm{L}}_{\mathrm{E}}$ and $\hat{\mathrm{p}}^{\mathrm{G}}_{\mathrm{E}}$ denote the effective parts of the direct production terms of momentum, which are defined as

$$\hat{\mathbf{p}}^{\mathrm{L}}_{\mathrm{E}} = -\gamma^{\mathrm{L}}_{\mathbf{w}_{\mathrm{LS}}} \mathbf{w}_{\mathrm{LS}} - \gamma^{\mathrm{L}}_{\mathbf{w}_{\mathrm{GS}}} \mathbf{w}_{\mathrm{GS}} \,, \qquad \hat{\mathbf{p}}^{\mathrm{G}}_{\mathrm{E}} = -\gamma^{\mathrm{G}}_{\mathbf{w}_{\mathrm{GS}}} \mathbf{w}_{\mathrm{GS}} - \gamma^{\mathrm{G}}_{\mathbf{w}_{\mathrm{LS}}} \mathbf{w}_{\mathrm{LS}} \,, \tag{15}$$

whereat the occurring material parameters are restricted by

$$\gamma^{\mathrm{L}}_{\mathbf{w}_{\mathrm{LS}}} \geq 0 \,, \qquad \gamma^{\mathrm{G}}_{\mathbf{w}_{\mathrm{GS}}} \geq 0 \,, \qquad \gamma^{\mathrm{L}}_{\mathbf{w}_{\mathrm{GS}}} + \gamma^{\mathrm{G}}_{\mathbf{w}_{\mathrm{LS}}} = 0 \,. \tag{16}$$

4 NUMERICAL EXAMPLE

In order to show the applicability of the developed model, a numerical simulation of a real experiment, cp. [30], is carried out. The dimensions of the specimen and the damaged virtual specimen are depicted in Figure 3. It is discretized with 142 linear eight-nodular brick elements and the total number of degrees of freedom is 2492. On both flanks a displacement of $\mathrm{u} = 0.6$ mm is applied in y-direction. Moreover, the boundary surface at the beginning of the notch is open for the gas phase, i.e., air can flow in and out.

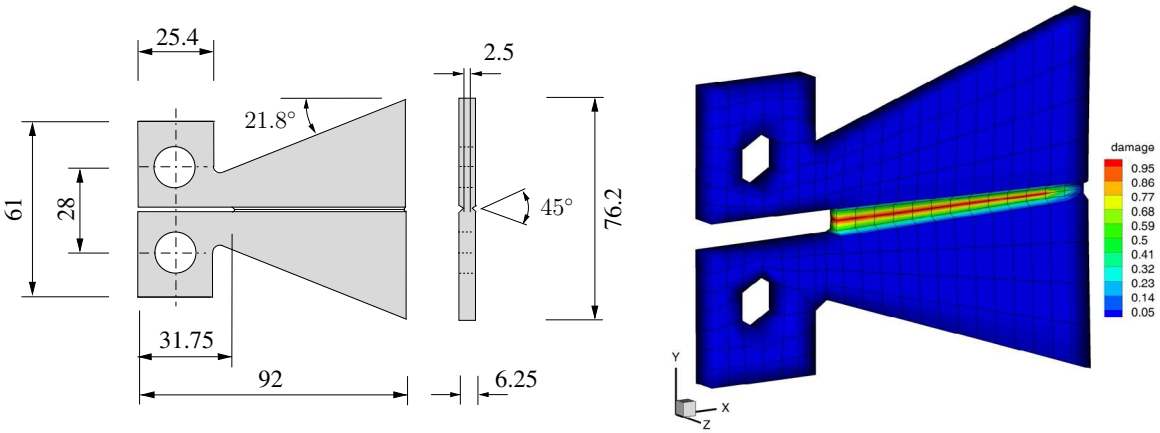

Figure 3: TDCB geometry, cp. [30] (left); damaged virtual specimen (right).

During the loading the TDCB fails. After the loading process the specimen is unloaded, because in the real experiment the specimen is able to heal, only if the crack faces come into

contact. Then, the TDCB gets 48 hours resting time before it is reloaded. As it is depicted in Figure 4, the results of the numerical simulation is qualitatively in a very good agreement to the experimental results of [30].

Table 1: Initial material parameters.

	S	H	L	G	C	unit
Young's modulus E^α	3.0e+9	3.0e+9	–	–	–	Pa
Poisson's ratio ν^α	0.2	0.2	–	–	–	–
real density $\rho^{\alpha\mathrm{R}}_{0\alpha}$	1200.0	980.0	980.0	1.0	–	kg/m^3
Darcy parameter k^α_{Darcy}	–	–	9.0e-9	5.0e+2	–	m^4/N s
Parameter associated with healing k^{L}_h	–	–	5.0e+1	–	–	Pa
initial volume fraction n^α	0.7	0.0	0.2	0.1	–	–
initial concentration c^α_0	–	–	–	–	1.0	$\times 100\%$
initial saturation $\mathrm{s}^{\mathrm{L}}_0$	–	–	0.9	–	–	–

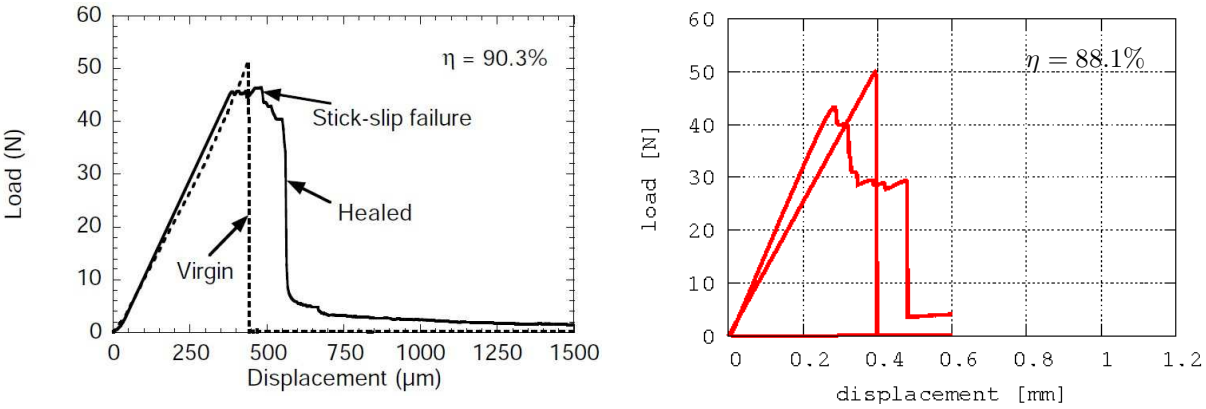

Figure 4: Experimental result, cp. [30] (left); result of the numerical simulation (right).

5 CONCLUSION

The presented work concentrates on the numerical simulation of damage as well as healing effects in a self-healing polymer composite. As the underlying theoretical framework the Theory of Porous Media is used. The developed multiphase model consists of the solid matrix material with dispersed catalysts, the liquid like healing agents, the solid like healed material, and the gas phase. For the separate description of damage for the solid and the healed material, two different damage functions are introduced based on the $(1 - D)$ approach. In order to describe the healing mechanism, a phase transition between the liquid healing agents and the solid healed material is considered.

To show the applicability of the developed model, the numerical simulation of a tapered double cantilever beam (TDCB) is compared with the experimental result from [30]. The simulation shows a qualitatively good agreement with the experimental observation, even for the healing efficiency. The divergence between both results can be explained, e.g., due to the fact that the healing of the real specimen depends on different factors, like wetting, different distributions of microcapsules and catalysts in the damaged area, etc.. Hence, it can be assumed that the resulting load-displacement curves of different specimens vary.

Acknowledgements This work has been supported by the German Research Society (DFG) within the Priority Program SPP 1568 "Design and Generic Principles of Self-healing Materials" under the grant number BL 417/7-1.

REFERENCES

[1] White, S.R., Sottos, N.R., Geubelle, P.H., Moore, J.S., Kessler, M.R., Sriram, S.R., Brown, E.N. and Viswanathan, S. Autonomic healing of polymer composites. *Nature* (2001) **409**:794–797.

[2] Grigoleit, S. *Überblick über Selbstheilende Materialien*. Tech. Report, Frauenhofer-Institut für Naturwissenschaftlich-Technische Trendanalysen (INT), (2011).

[3] Yuan, Y.C., Yin, T., Rong, M.Z. and Zhang, M.Q. Self healing polymers and polymer composites. Concept, realization and outlook: a review. *eXPRESS Polymer Letters* (2008) **2**:238–250.

[4] Hager, M.D., Greil, P., Leyens, C., van der Zwaag, S. and Schubert, U.S. Self-healing materials. *Advanced Materials* (2010) **22**:5424–5430.

[5] Zemskov, S.V., Jonkers, H.M. and Vermolen, F.J. Two analytical models for the probability characteristics of a crack hitting encapsulated particles: application to self-healing materials. *Computational Materials Science* (2011) **50**:3323–3333.

[6] Sanada, K., Itaya, N. and Shindo, Y. Self-healing of interfacial debonding in fiber-reinforced polymers and effect of microstructure on strength recovery. *The Open Mechanical Engineering Journal* (2008) **2**:97–103.

[7] Barbero, E.J. and Ford, K.J. Characterization of self-healing fiber-reinforced polymer-matrix composite with distributed damage. *Journal of Advanced Materials* (2007) **39**:20–27.

[8] Privman, V., Dementsov, A. and Sokolov, I. Modeling of self-healing polymer composites reinforced with nanoporous glass fibers. *Journal of Computational and Theoretical Nanoscience* (2007) **4**:190–193.

[9] Voyiadjis, G.Z., Shojaei, A. and Li, G. A thermodynamic consistent damage and healing model for self healing materials. *International Journal of Plasticity* (2011) **27**:1025–1044.

[10] Yagimli, B. and Lion, A. Experimental investigations and material modelling of curing processes under small deformations. *Zeitschrift fr angewandte Mathematik und Mechanik* (2011) **91**:342–359.

[11] Schimmel, E.C. and Remmers, J.J.C. *Development of a constitutive model for self-healing materials*. Tech. Report, Delft Aerospace Computational Science, (2006).

[12] Voyiadjis, G.Z., Shojaei, A., Li, G. and Kattan, P.I. A theory of anisotropic healing and damage mechanics of materials. *Proceedings of the Royal Society London A* (2012) **468**:163–183.

[13] Mergheim, J. and Steinmann, P. Phenomenological modelling of self-healing polymers based on integrated healing agents. *Computational Mechanics* (2013) **52**:681–692.

[14] Henson, G.M. Engineering models for synthetic vascular materials with interphase mass, momentum and heat transfer. *International Journal of Solids and Structures* (2012), **50**:2371–2382.

[15] Bowen, R.M. Incompressible porous media models by use of the theory of mixtures. *International Journal of Engineering Science* (1980) **18**:1129–1148.

[16] Bowen, R.M. Compressible porous media models by use of the theory of mixtures. *International Journal of Engineering Science* (1982) **20**:697–735.

[17] de Boer, R. *Trends in continuum mechanics of porous media*. Springer, (2005).

[18] de Boer, R. *Theory of porous media*. Springer, (2000).

[19] Ehlers, W. *Poröse Medien - ein kontinuummechanisches Modell auf der Basis der Mischungstheorie*. PhD.-Thesis, Universität - Gesamthochschule - Essen, (1989).

[20] Ehlers, W. and Bluhm, J. *(ed.)*, *Porous media*. Springer, (2002).

[21] Ateshian, G.A. and Ricken, T. Multigenerational interstitial growth of biological tissues. *Biomechanics and Modelling in Mechanobiology* (2010) **9**:689–702.

[22] Hunphrey, J. and Rajagopal, K. A constrained mixture model for growth and remodelling of soft tissues. *Mathematical Models and Methods in Applied Science* (2002) **12**:407–430.

[23] Rodriguez, E., Hoger, A. and McCulloch, A. Stress-dependent finite growth in soft elastic tissues. *Journal of Biomechanics* (1994) **27**:455–467.

[24] Bluhm, J., Specht, S., Schröder, J. Modeling of self-healing effects in polymeric composites. *Archive of Applied Mechanics* (2014) *DOI 10.1007/s00419-014-0946-7*.

[25] Kachanov, L.M. Time of the rupture process under creep conditions. *Izvestija Akademii Nauk Sojuza Sovetskich Socialisticeskich Republiki (SSSR) Otdelenie Techniceskich Nauk (Moskra)* (1958) **8**:26–31.

[26] Miehe, C. Discontinuous and continuous damage evolution in Ogden-type large-strain elastic materials. *European Journal of Mechanics, A/Solids* (1995) **14**:697–720.

[27] Balzani, D. *Polyconvex anisotropic energies and modeling of damage applied to arterial walls*. PhD.-Thesis, Universität Duisburg-Essen, (2006).

[28] Bluhm, J., Ricken, T. and Bloßfeld, W.M. Ice formation in porous media, in *Advances in extendet & multifield theories for continua*. Markert, B. *(ed.)* Springer, (2011).

[29] Michalowski, R.L. and Zhu, M. Frost heave modelling using porosity rate function. *International Journal for Numerical and Analytical Methods in Geomechanics* (2006) **30**:703–722.

[30] Brown, E.N., Sottos, N.R. and White, S.R. Fracture testing of a self-healing polymer composite. *Experimental Mechanics* (2002) **42**:372–379.